


**Single quantum emitters with spin ground states based on Cl bound excitons in ZnSe**Aziz Karasahin,<sup>1,\*</sup> Robert M. Pettit,<sup>1,2</sup> Nils von den Driesch,<sup>3,4</sup> Marvin Marco Jansen <sup>3,4</sup>  
Alexander Pawlis,<sup>3,4</sup> and Edo Waks<sup>1,†</sup><sup>1</sup>*Institute for Research in Electronics and Applied Physics, Department of Electrical and Computer Engineering and Joint Quantum Institute, University of Maryland, College Park, Maryland 20742, USA*<sup>2</sup>*Intelligence Community Postdoctoral Research Fellowship Program, University of Maryland, College Park, Maryland 20742, USA*<sup>3</sup>*Peter-Grünberg-Institute (PGI-9), Forschungszentrum Jülich GmbH, 52425 Jülich, Germany*<sup>4</sup>*JARA-FIT (Fundamentals of Future Information Technology), Jülich-Aachen Research Alliance, 52062 Aachen, Germany*

(Received 10 March 2022; accepted 15 August 2022; published 19 September 2022)

Defects in wide-band-gap semiconductors are promising qubit candidates for quantum communication and computation. Epitaxially grown II-VI semiconductors are particularly promising host materials due to their direct band gap and potential for isotopic purification to a spin-zero nuclear background. Here, we show an alternative type of single photon emitter with potential electron spin qubits based on Cl impurities in ZnSe. We utilize a quantum well to increase the binding energies of donor emission and confirm single photon emission with short radiative lifetimes of 192 ps. Furthermore, we verify that the ground state of the Cl donor complex contains a single electron by observing two-electron-satellite emission, leaving the electron in higher orbital states. We also characterize the Zeeman splitting of the exciton transition by performing polarization-resolved magnetic spectroscopy on single emitters. Our results suggest single Cl impurities are suitable as a single photon source with a potential photonic interface.

DOI: [10.1103/PhysRevA.106.L030402](https://doi.org/10.1103/PhysRevA.106.L030402)**I. INTRODUCTION**

Impurities [1] in wide-band-gap semiconductors are an essential building block for quantum photonic devices [1–3]. These isolated impurities generate single photons that exhibit transform-limited linewidths [4,5] and small inhomogeneous broadening [6,7] through their radiative optical transitions. They also provide isolated bound electrons [8] or holes [9] that can serve as spin-photon interfaces with long coherence times [10,11]. Furthermore, semiconductor fabrication and integration methods allow efficient spin-photon interfaces [12–14]. Hence, these platforms could satisfy major requirements of scalable quantum technology by combining pristine radiative properties with long-coherence time spin qubits in a practical setting.

Zinc selenide (ZnSe) is an appealing material as the host crystal because it possesses a direct optical band gap of 2.8 eV and a large natural abundance of nuclear spin-0 isotopes. The direct band gap allows efficient radiative transitions that can generate bright excitonic emission. Both single fluorine (F) donors [15] and single nitrogen (N) acceptors [9] have been optically isolated in this host material. Ensemble measurements have also revealed the potential for optically active spin qubits [16]. Recently, the growth of isotopically purified (Zn,Mg)Se/ZnSe quantum well structures was also demonstrated [17]. Spin purification of the host crystal further resulted in extended spin coherence times [18]. Moreover,

donor-bound excitons in nanostructured pillars have been used to demonstrate indistinguishable single photon emission between two independent emitters [6], two-photon entanglement [7], and optical pumping of the donor spin [19].

Most studies on impurity-bound exciton emission in ZnSe have focused on the fluorine (F) impurity, which possesses a nuclear spin of 1/2 and a smaller atomic radius compared to selenium (Se) atoms. The small radius causes self-compensation and is expected to lead to more complex defect formation in the host lattice [20]. On the other hand, chlorine (Cl) has an atomic radius closer to that of Se and is therefore more suitable as a dopant with a low probability of self-compensation [21]. This enables Cl doping levels that cover a wide range of densities between  $10^{16}$  and  $10^{19}$  cm<sup>-3</sup>. But all past work on Cl impurity-bound exciton emission was in the large ensemble regime, and single Cl donor-bound exciton emission has yet to be studied. Additionally, Cl has a nuclear spin of 3/2 and therefore offers distinct opportunities with respect to F for coupling to the nuclear spin degree of freedom.

**II. RESULTS**

Here, we isolate single Cl impurities in ZnSe and show that they act as an efficient single photon source with a potential to act as a spin qubit. Optical isolation of single bound excitons requires a sufficiently low density of impurity atoms and sufficiently large exciton binding energy to separate bound exciton emission from the free exciton emission. We achieve these requirements by using a quantum well that is delta doped with a low concentration of Cl impurities. Quantum confinement

\*azizk@umd.edu

†edowaks@umd.edu

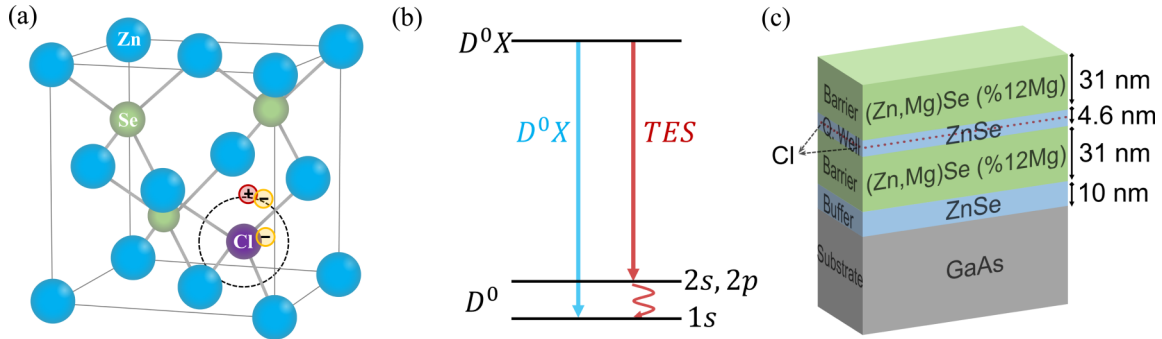


FIG. 1. (a) Crystal structure of ZnSe with a single Cl impurity replacing a Se atom. (b) Energy band diagram showing the ground state ( $D^0$ ) and excited state ( $D^0X$ ), along with the bound exciton and two-electron-satellite emission, shown as blue and red arrows. (c) Layer structure of the grown material with *in situ* doped Cl impurities in the ZnSe quantum well.

on the order of the Bohr radius of the bound exciton results in an increase in the exciton binding energy and therefore allows us to better separate the free exciton and bound exciton emission in energy [22–24]. We show fast and stable single photon emission from single Cl donor-bound excitons. We also confirm the existence of a single electron ground state by observing two-electron-satellite transitions and observing the Zeeman splitting with the application of a magnetic field in the Faraday geometry. These results establish Cl impurities in ZnSe as a promising optically active qubit system.

Figure 1(a) illustrates the atomic structure of a ZnSe crystal with a single Cl impurity. In its intrinsic form, zinc and selenium atoms are arranged in a face-centered-cubic lattice where each zinc atom is surrounded by four selenium atoms. A single Cl impurity replaces a Se atom [20,25] when chlorine impurities are introduced into the lattice via *in situ* doping or ion implantation. The Cl impurity serves as a neutral electron donor, consisting of the positively charged chlorine core and an additional single bound electron, shown in Fig. 1(a). This extra donor-bound electron may serve as a stable single photon emitter with an electron spin ground state.

Figure 1(b) shows the level structure of the Cl impurity. Optical excitation above the ZnSe band gap produces free excitons in the quantum well. These excitons can become bound to the Cl impurity, forming an impurity-bound exciton state ( $D^0X$ ). This state can radiatively decay back to the donor electron  $1s$  ground state, emitting a photon around 440 nm. The bound exciton can also recombine and leave the donor electron in the higher-energy  $2s, 2p$  states through an Auger recombination process, emitting a longer-wavelength photon. The observation of two-electron satellites establishes the presence of an electron ground state.

Figure 1(c) shows the epitaxial layer structure of the sample used in this work. The sample is composed of a 4.6-nm ZnSe quantum well embedded in a  $(\text{Zn}_{0.88}\text{Mg}_{0.12})\text{Se}$  barrier on the top and bottom, each with a thickness of 31 nm. To achieve controlled doping of impurities while sustaining the high crystalline quality, we grow a thin Cl delta-doped layer in the middle of the ZnSe quantum well. The delta-doped layer has a Cl sheet concentration of approximately  $10^9 \text{ cm}^{-2}$ . The overall structure was grown on a GaAs substrate covered with a 10-nm ZnSe buffer layer.

We performed optical measurements with a home-built confocal microscope using an objective with a numerical aper-

ture of 0.82. We mounted samples on an XYZ piezo stage and maintained the sample temperature at 3.6 K in a closed-loop helium cryostat. A 405-nm wavelength continuous-wave diode laser, whose energy is larger than the band gaps of the barrier and the quantum well, was used for excitation. We analyzed the photoluminescence signal with an imaging spectrometer (Princeton Instruments, SP-2750) with a spectral resolution of 15 pm or single photon detectors (Micro Photon Devices, PDM series). To optically isolate individual impurities in the bulk material, we used confocal collection to a single-mode fiber.

The photoluminescence spectrum from the sample is shown in Fig. 2(a). We observed broad emission from the heavy-hole free exciton (labeled as  $FX$ , centered at 436.7 nm) and negatively charged trion ( $X^-$ ) in the quantum well [26]. In addition to these lines, we observed a sharp localized emission line at 440.4 nm from excitons bound to neutral donors ( $D^0X$ ). As we move the position of the sample, we observe different localized lines appearing in the spectrum at different spectral locations. In contrast, the energy of free exciton and trion lines remains constant throughout the sample. Figure 2(b) shows an image of the photoluminescence from a representative  $D^0X$  line, recorded by filtering the sample photoluminescence through a bandpass filter centered at 441 nm with a passband of about 1 nm, demonstrating the spatially localized nature of the  $D^0X$  emission.

Figure 2(c) plots a histogram of the energies of 29 emission lines acquired at different locations in the sample relative to the free exciton emission. The mean distribution of the emissions is shifted by 15 meV relative to the free exciton line. This binding energy is reasonable assuming a similar Bohr radius (about 3 nm) for the free exciton and bound exciton, leading to about a two to three times increase in the  $D^0X$  binding energy compared to reported bulk values of 7 meV [27]. Using the distribution of emission energies, we calculate the standard deviation of the binding energy as 6 meV. The observed inhomogeneous broadening is possibly caused by fluctuations of the donor positions within the well, local thickness fluctuations of the quantum well, and local strain variations [28,29].

To verify that the observed  $D^0X$  emission originates from a bound state of the quantum well free exciton, we perform a photoluminescence excitation measurement. We use a tunable laser with a fixed pump power of 100 nW. We tune the laser

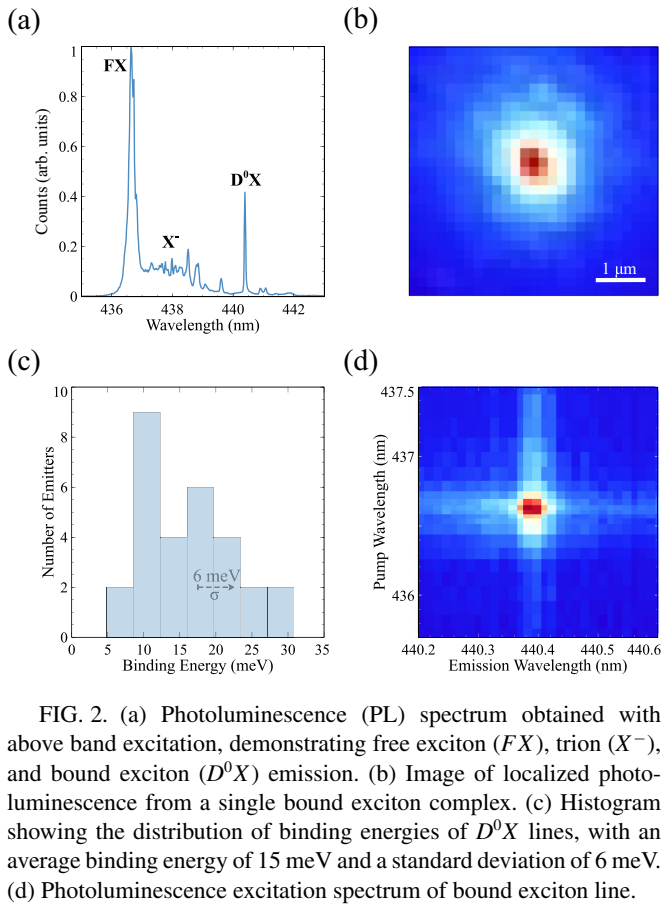


FIG. 2. (a) Photoluminescence (PL) spectrum obtained with above band excitation, demonstrating free exciton ( $FX$ ), trion ( $X^-$ ), and bound exciton ( $D^0X$ ) emission. (b) Image of localized photoluminescence from a single bound exciton complex. (c) Histogram showing the distribution of binding energies of  $D^0X$  lines, with an average binding energy of 15 meV and a standard deviation of 6 meV. (d) Photoluminescence excitation spectrum of bound exciton line.

emission over the free exciton line and monitor the emission from a  $D^0X$  line. In the absence of an above-barrier laser, a moderately  $n$ -doped quantum well has been shown to develop a low-density hole gas. Applying an appropriate above-barrier laser supplies a sufficient electron concentration in the quantum well [30–32]. During this measurement, we inject a weak above-barrier laser (about 3 nW at 405 nm) in addition to the pump laser. At this power, the above-barrier laser produces negligible photoluminescence for the integration times used, however, it helps control the carrier densities in the quantum well. Figure 2(d) shows the photoluminescence excitation spectrum of a  $D^0X$  line as we tune the pump laser over the free exciton line. We observe strong emission from the  $D^0X$  line when the laser is resonant with the free exciton. This enhancement suggests that free excitons in the quantum well nonradiatively relax to form donor-bound excitons at the impurity.

Figure 3 shows the observation of two-electron-satellite emission in the presence of resonant excitation, which can be used as an additional tool to identify donor-bound exciton emission. The top panel shows the PL signal obtained with a weak above-barrier laser while varying the power of a resonant pump laser tuned to the  $D^0X$  line. In this measurement the counts contributed by the above-barrier laser are no longer negligible due to the longer integration times used. Two-electron-satellite (TES) emission 19.6 meV below the  $D^0X$  line emerges, and its intensity increases as we increase the resonant pump power, shown in Fig. 3(a). Satellite emission

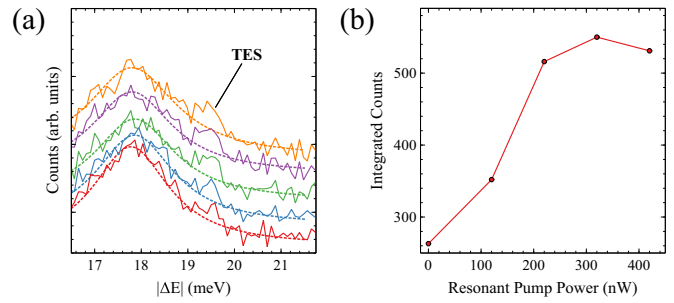


FIG. 3. (a) Spectra showing the TES line with increasing resonant pump power. The horizontal axis represents energy separation below the  $D^0X$  line. Spectra are offset for clarity. Dashed lines represent the background used to integrate the TES emission. (b) Background-corrected and integrated counts from the TES line.

appears lower in energy by an amount equal to the spacing of the  $n = 1$  and  $n = 2$  orbitals of the  $D^0$  electron determined by a hydrogenic donor model as illustrated in Fig. 1(b). The observed 19.6 meV separation between the TES line and the  $D^0X$  line is consistent with past studies on chlorine donors in ZnSe [27]. The weak nature of this emission is due to the predominant relaxation of the  $D^0X$  state to the  $1s$  ground state of the donor electron. The background-corrected integrated intensities of the observed TES line with increasing resonant pump power show saturation, shown in Fig. 3(b). The observation of two-electron-satellite emission supports the presence of an electron ground state, which may be useful as a potential spin qubit.

To confirm that the emission originates from a two-level system, we perform intensity-dependent photoluminescence measurements. Figure 4(a) shows the emission intensity of both the free exciton and bound exciton line as a function of pump intensity. The bound exciton line exhibits an emission intensity saturation at pump powers above  $5 \mu\text{W}$ . In contrast, the free exciton line exhibits no saturation behavior. The inset of the figure shows the log scale power dependence of both curves. Both  $D^0X$  and  $FX$  lines are fitted for excitation powers up to  $1 \mu\text{W}$ , showing nearly linear dependence on the excitation power, with  $P^{0.98}$  and  $P^{1.06}$ , respectively.

In order to demonstrate single photon emission, we perform second-order correlation measurements using a beam

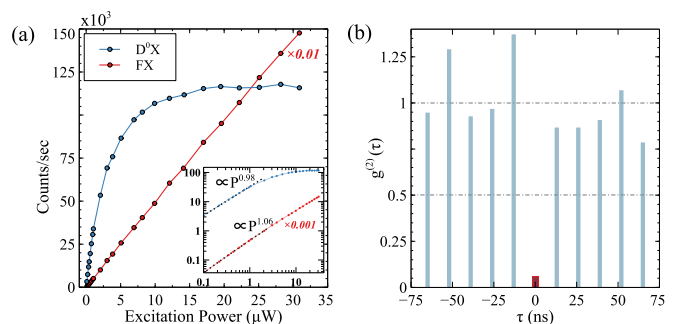


FIG. 4. (a) Power-dependent emission intensity of the bound exciton (blue) and free exciton (red). The inset shows a log scale view of the data. (b) Second-order autocorrelation function obtained from the  $D^0X$  line, demonstrating single photon emission.

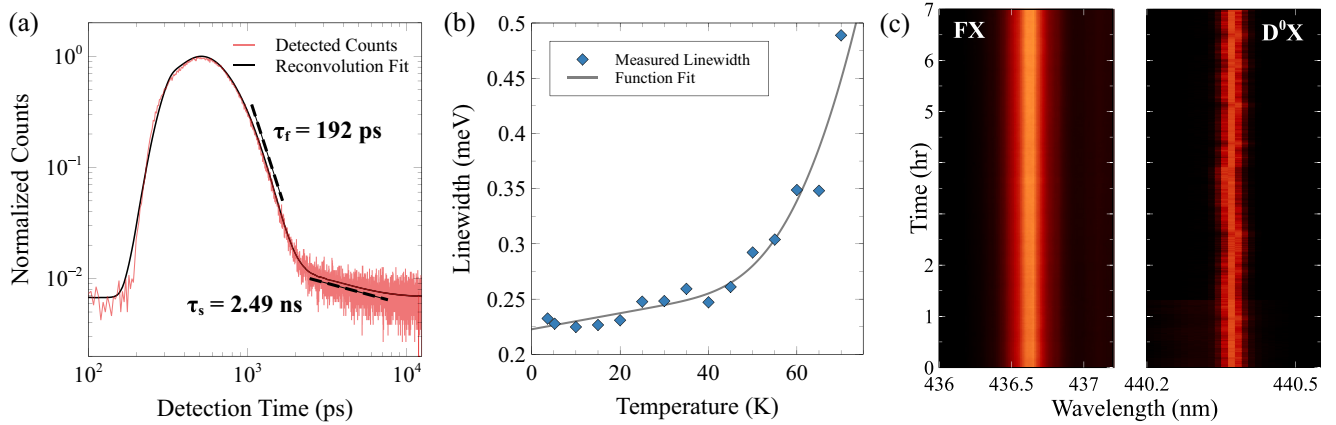


FIG. 5. (a) Time-resolved photoluminescence measurement showing a biexponential decay with dominant fast decay component of 192 ps and slow decay component of 2.49 ns. (b) Linewidth of the  $D^0X$  emission recorded as a function of temperature. (c) PL intensity recorded over 7 h showing the stability of the emitter.

splitter and two single photon detectors. To confirm that the emission is due to a single quantum emitter, we studied the photon statistics of the  $D^0X$  line. Figure 4(b) shows the results of the second-order autocorrelation measurements performed on the single line. We used a frequency-doubled Ti:sapphire laser emitting at 405 nm with a pulse repetition rate of 76 MHz to excite the emitters. Then, we coupled the collected emission to a single-mode fiber to have spatial filtering. The spectral filtering is performed by using narrow slits and a monochromator. Noise contributions from unfiltered background emission and detector dark counts are subtracted [33]. The second-order correlation exhibits clear antibunching with  $g^{(2)} = 0.06$ , which confirms that the emission line corresponds to a single photon emitter.

To characterize the donor-bound exciton state's lifetime, we perform time-resolved fluorescence measurements using 3 ps optical pulses. The  $D^0X$  emission is recorded by a single photon detector with timing jitter on the order of 100 ps. Figure 5(a) shows the histogram of photon arrival times obtained from a single bound exciton along with the biexponential decay fit. To mitigate the slow timing response of the detectors, we reconvolved (EASYTAU software, PicoHarp) the detector impulse response recorded at the  $D^0X$  emission wavelength with a custom-defined decay function. We extracted the parameters of the decay function by fitting the reconvolved function to the measured data. Extracted data show a biexponential decay, with a dominant fast decay time of 192 ps and a weak contribution from a slower component with a decay time of 2.49 ns. The fast decay time is consistent with previously reported values for other group-7 impurities in ZnSe [27] and indicates the possibility of realizing a bright and efficient single photon interface with chlorine donor-bound excitons in ZnSe. The origin of the slow component may be caused by the repopulation of the  $D^0X$  state from longer-lived nearby trapping states and is a matter of further investigation.

Figure 5(b) shows the temperature dependence of the  $D^0X$  linewidth up to 70 K. The measured linewidth is well described by a model,

$$\Gamma(T) = \Gamma_0 + aT + b[\exp(h\nu_{LO}/k_B T) - 1]^{-1}, \quad (1)$$

that describes the broadening of the bound exciton linewidth due to interactions with acoustic and optical phonons [34]. In the model  $\Gamma_0$  is the zero-temperature linewidth,  $a$  quantifies the coupling to acoustic phonons,  $b$  quantifies the coupling to longitudinal optical phonons, and  $h\nu_{LO}$  is the longitudinal optical phonon energy. For ZnSe,  $h\nu_{LO} = 31.8$  meV, and from the fit we determine  $\Gamma_0 = 223$   $\mu$ eV,  $a = 0.727$   $\mu$ eV/T, and  $b = 34.0$  meV. The zero-temperature linewidth of  $\Gamma_0/h = 53.9$  GHz is a factor of 65 larger than the expected lifetime-limited linewidth of 830 MHz given by  $1/(2\pi \cdot \tau)$ , where  $\tau$  is the emitter lifetime. Further improvements to the observed linewidth could be found using resonant excitation of the  $D^0X$  which reduces the density of free charge carriers in the vicinity of the bound exciton.

Figure 5(c) highlights the long-term stability of the  $D^0X$ . The figure plots the photoluminescence spectrum over 7 h under continuous above-barrier excitation. The emission does not display any blinking, though slow spectral wandering is observed over a timescale of hours. We calculated the standard deviation of the spectral wandering to be 0.009 nm or  $\sim 14$  GHz, which is of the same order as our spectrometer resolution and less than the observed linewidth. The observed spectral wandering is about a factor of 17 larger than the lifetime-limited linewidth and may also be further improved with resonant excitation of the  $D^0X$ . These results demonstrate the potential for developing stable sources of single photons with chlorine donor-bound excitons in ZnSe.

To investigate the spin properties of the bound exciton complex, we performed magnetophotoluminescence measurements on the  $D^0X$  line for magnetic fields up to 9 T applied along the growth direction (Faraday geometry). The optically allowed transitions in this configuration are presented in Fig. 6(a). The total spin of the bound exciton ground state is given by the single spin-1/2 electron. In the bound exciton excited state, the donor electron forms a spin singlet with the electron of the exciton, giving a total spin determined by the spin-3/2 heavy hole [35]. For increasing magnetic field, two orthogonally polarized circular emission lines emerge as expected, shown in Fig. 6(b). Spectra indicated by solid (dashed) lines are recorded for  $\sigma^+$  ( $\sigma^-$ ) polarization. The energy difference of the two allowed transitions is

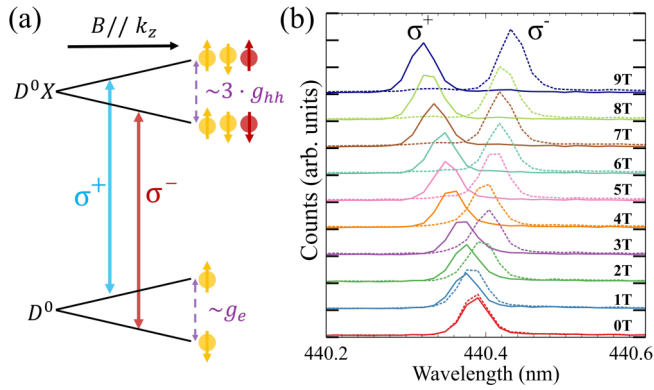


FIG. 6. (a) Optical selection rules under applied out-of-plane magnetic field. (b) Polarization-resolved photoluminescence spectrum recorded at increasing magnetic field intensity, showing the splitting into orthogonal circular polarizations.

proportional to  $g_{\text{eff}} = g_e - 3g_{\text{hh}}$ . From the observed energy splitting between those two transitions, we infer  $g_{\text{eff}} = 0.9$  which is in good agreement with previous results obtained from single fluorine donors in ZnSe [15]. Additionally, we observe a diamagnetic shift of the  $D^0X$  emission of  $3.25 \mu\text{eV}/\text{T}^2$ . The lack of fine structure splitting and the clear splitting into orthogonal circular polarizations are consistent with the expected Kramer's degeneracy of the neutral donor state containing a single electron in its ground state [35].

### III. CONCLUSION

In conclusion, we demonstrated that excitons bound to single Cl donor atoms in ZnSe quantum wells can serve as bright and stable single photon sources. Emission of the bound

excitons exhibited clear saturation and single photon emission was confirmed by observing photon antibunching. The fast radiative recombination time below 200 ps demonstrates the possibility of realizing a single photon source with a brightness comparable to state-of-the-art quantum dots. Coupling donor atoms to photonic structures can further decrease the lifetime and lead to high-cooperativity cavities. Observation of two-electron-satellite and circularly polarized emission under a Faraday magnetic field indicates a single electron ground state which could be employed for spin-qubit applications. Isotopic purification of the host crystal to be nuclear spin free makes Cl impurities an attractive candidate for long-lived memory qubits [17] and provides a route towards optically bright spin qubits with long coherence times. These unique aspects could allow a wide range of applications in quantum information processing.

### ACKNOWLEDGMENTS

This work is supported by the Air Force Office of Scientific Research (Grant No. FA95502010250), The Maryland-ARL Quantum Partnership (Grant No. W911NF1920181), and Deutsche Forschungsgemeinschaft (DFG, German Research Foundation) under Germany's Excellence Strategy-Cluster of Excellence Matter and Light for Quantum Computing (ML4Q) (EXC 2004 1-390534769). R.M.P. acknowledges support through an appointment to the Intelligence Community Postdoctoral Research Fellowship Program at the University of Maryland, administered by Oak Ridge Institute for Science and Education through an interagency agreement between the U.S. Department of Energy and the Office of the Director of National Intelligence.

- [1] D. D. Awschalom, R. Hanson, J. Wrachtrup, and B. B. Zhou, Quantum technologies with optically interfaced solid-state spins, *Nat. Photonics* **12**, 516 (2018).
- [2] G. Wolfowicz, F. J. Heremans, C. P. Anderson, S. Kanai, H. Seo, A. Gali, G. Galli, and D. D. Awschalom, Quantum guidelines for solid-state spin defects, *Nat. Rev. Mater.* **6**, 906 (2021).
- [3] J. R. Weber, W. F. Koehl, J. B. Varley, A. Janotti, B. B. Buckley, C. G. Van De Walle, and D. D. Awschalom, Quantum computing with defects, *Proc. Natl. Acad. Sci. USA* **107**, 8513 (2010).
- [4] M. E. Trusheim, B. Pingault, N. H. Wan, M. Gündoğan, L. De Santis, R. Debroux, D. Gangloff, C. Purser, K. C. Chen, M. Walsh, J. J. Rose, J. N. Becker, B. Lienhard, E. Bersin, I. Paradeisanos, G. Wang, D. Lyzwa, A. R. Montblanch, G. Malladi, H. Bakhru, A. C. Ferrari, I. A. Walmsley, M. Atatüre, and D. Englund, Transform-Limited Photons From a Coherent Tin-Vacancy Spin in Diamond, *Phys. Rev. Lett.* **124**, 023602 (2020).
- [5] C. Bradac, W. Gao, J. Forneris, M. E. Trusheim, and I. Aharonovich, Quantum nanophotonics with group IV defects in diamond, *Nat. Commun.* **10**, 5625 (2019).
- [6] K. Sanaka, A. Pawlis, T. D. Ladd, K. Lischka, and Y. Yamamoto, Indistinguishable Photons from Independent Semiconductor Nanostructures, *Phys. Rev. Lett.* **103**, 053601 (2009).
- [7] K. Sanaka, A. Pawlis, T. D. Ladd, D. J. Sleiter, K. Lischka, and Y. Yamamoto, Entangling single photons from independently tuned semiconductor nanoemitters, *Nano Lett.* **12**, 4611 (2012).
- [8] X. Linpeng, M. L. K. Viitaniemi, A. Vishnuradhan, Y. Kozuka, C. Johnson, M. Kawasaki, and K.-M. C. Fu, Coherence Properties of Shallow Donor Qubits in Zn O, *Phys. Rev. Appl.* **10**, 064061 (2018).
- [9] S. Strauf, P. Michler, M. Klude, D. Hommel, G. Bacher, and A. Forchel, Quantum Optical Studies on Individual Acceptor Bound Excitons in a Semiconductor, *Phys. Rev. Lett.* **89**, 177403 (2002).
- [10] D. D. Sukachev, A. Sipahigil, C. T. Nguyen, M. K. Bhaskar, R. E. Evans, F. Jelezko, and M. D. Lukin, Silicon-Vacancy Spin Qubit in Diamond: A Quantum Memory Exceeding 10 ms with Single-Shot State Readout, *Phys. Rev. Lett.* **119**, 223602 (2017).
- [11] X. Linpeng, T. Karin, M. V. Durnev, M. M. Glazov, R. Schott, A. D. Wieck, A. Ludwig, and K.-M. C. Fu, Optical spin control and coherence properties of acceptor bound holes in strained GaAs, *Phys. Rev. B* **103**, 115412 (2021).
- [12] M. Atatüre, D. Englund, N. Vamivakas, S. Y. Lee, and J. Wrachtrup, Material platforms for spin-based photonic quantum technologies, *Nat. Rev. Mater.* **3**, 38 (2018).

- [13] Z. Luo, S. Sun, A. Karasahin, A. S. Bracker, S. G. Carter, M. K. Yakes, D. Gammon, and E. Waks, A spin-photon interface using charge-tunable quantum dots strongly coupled to a cavity, *Nano Lett.* **19**, 7072 (2019).
- [14] A. Javadi, D. Ding, M. H. Appel, S. Mahmoodian, M. C. Löbl, I. Söllner, R. Schott, C. Papon, T. Pregolato, S. Stobbe, L. Midolo, T. Schröder, A. D. Wieck, A. Ludwig, R. J. Warburton, and P. Lodahl, Spin-photon interface and spin-controlled photon switching in a nanobeam waveguide, *Nat. Nanotechnol.* **13**, 398 (2018).
- [15] K. De Greve, S. M. Clark, D. Sleiter, K. Sanaka, T. D. Ladd, M. Panfilova, A. Pawlis, K. Lischka, and Y. Yamamoto, Photon antibunching and magnetospectroscopy of a single fluorine donor in ZnSe, *Appl. Phys. Lett.* **97**, 241913 (2010).
- [16] A. Greilich, A. Pawlis, F. Liu, O. A. Yugov, D. R. Yakovlev, K. Lischka, Y. Yamamoto, and M. Bayer, Spin dephasing of fluorine-bound electrons in ZnSe, *Phys. Rev. B* **85**, 121303 (2012).
- [17] A. Pawlis, G. Mussler, C. Krause, B. Bennemann, U. Breuer, and D. Grutzmacher, MBE growth and optical properties of isotopically purified ZnSe heterostructures, *ACS Appl. Electron. Mater.* **1**, 44 (2019).
- [18] E. Kirstein, E. A. Zhukov, D. S. Smirnov, V. Nedelea, P. Greve, I. V. Kalitukha, V. F. Sapega, A. Pawlis, D. R. Yakovlev, M. Bayer, and A. Greilich, Extended spin coherence of the zinc-vacancy centers in ZnSe with fast optical access, *Commun. Mater.* **2**, 91 (2021).
- [19] D. J. Sleiter, K. Sanaka, Y. M. Kim, K. Lischka, A. Pawlis, and Y. Yamamoto, Optical pumping of a single electron spin bound to a fluorine donor in a ZnSe nanostructure, *Nano Lett.* **13**, 116 (2013).
- [20] L. S. dos Santos, W. G. Schmidt, and E. Rauls, Group-VII point defects in ZnSe, *Phys. Rev. B* **84**, 115201 (2011).
- [21] K. Ohkawa, T. Mitsuyu, and O. Yamazaki, Characteristics of Cl-doped ZnSe layers grown by molecular-beam epitaxy, *J. Appl. Phys.* **62**, 3216 (1987).
- [22] H. Mariette, F. Dalbo, N. Magnea, G. Lentz, and H. Tuffigo, Optical investigation of confinement and strain effects in CdTe/Cd<sub>1-x</sub>Zn<sub>x</sub>Te single quantum wells, *Phys. Rev. B* **38**, 12443 (1988).
- [23] A. V. Kavokin, V. P. Kochereshko, G. R. Posina, I. N. Uraltsev, D. R. Yakovlev, G. Landwehr, R. N. Bicknell-Tassius, and A. Waag, Effect of the electron Coulomb potential on hole confinement in II-VI quantum wells, *Phys. Rev. B* **46**, 9788 (1992).
- [24] A. Pawlis, T. Berstermann, C. Brüggemann, M. Bombeck, D. Dunker, D. R. Yakovlev, N. A. Gippius, K. Lischka, and M. Bayer, Exciton states in shallow ZnSe/(Zn,Mg)Se quantum wells: Interaction of confined and continuum electron and hole states, *Phys. Rev. B* **83**, 115302 (2011).
- [25] S. Pöykkö, M. J. Puska, and R. M. Nieminen, Chlorine-impurity-related defects in ZnSe, *Phys. Rev. B* **57**, 12164 (1998).
- [26] O. Homburg, K. Sebald, P. Michler, J. Gutowski, H. Wenisch, and D. Hommel, Negatively charged trion in ZnSe single quantum wells with very low electron densities, *Phys. Rev. B* **62**, 7413 (2000).
- [27] P. J. Dean, D. C. Herbert, C. J. Werkhoven, B. J. Fitzpatrick, and R. N. Bhargava, Donor bound-exciton excited states in zinc selenide, *Phys. Rev. B* **23**, 4888 (1981).
- [28] F. A. P. Osorio, M. H. Degani, and O. Hipolito, Bound impurity in GaAs-Ga<sub>1-x</sub>Al<sub>x</sub>As quantum-well wires, *Phys. Rev. B* **37**, 1402 (1988).
- [29] R. T. Senger and K. K. Bajaj, Binding energies of excitons in II-VI compound-semiconductor based quantum well structures, *Phys. Status Solidi B* **241**, 1896 (2004).
- [30] J. Puls, G. V. Mikhailov, S. Schwertfeger, D. R. Yakovlev, F. Henneberger, and W. Faschinger, High-excitation effects in the optical properties of  $\delta$ -doped ZnSe quantum wells, *Phys. Status Solidi B* **227**, 331 (2001).
- [31] M. Hayne, A. Usher, A. S. Plaut, and K. Ploog, Optically induced density depletion of the two-dimensional electron system in GaAs/Al<sub>x</sub>Ga<sub>1-x</sub>As heterojunctions, *Phys. Rev. B* **50**, 17208 (1994).
- [32] E. A. Zhukov, A. Greilich, D. R. Yakovlev, K. V. Kavokin, I. A. Yugova, O. A. Yugov, D. Suter, G. Karczewski, T. Wojtowicz, J. Kossut, V. V. Petrov, Y. K. Dolgikh, A. Pawlis, and M. Bayer, All-optical NMR in semiconductors provided by resonant cooling of nuclear spins interacting with electrons in the resonant spin amplification regime, *Phys. Rev. B* **90**, 085311 (2014).
- [33] J. H. Kim, C. J. Richardson, R. P. Leavitt, and E. Waks, Two-photon interference from the far-field emission of chip-integrated cavity-coupled emitters, *Nano Lett.* **16**, 7061 (2016).
- [34] I. Favero, G. Cassabois, R. Ferreira, D. Darson, C. Voisin, J. Tignon, C. Delalande, G. Bastard, P. Roussignol, and J. M. Gérard, Acoustic phonon sidebands in the emission line of single InAs/GaAs quantum dots, *Phys. Rev. B* **68**, 233301 (2003).
- [35] M. Bayer, G. Ortner, O. Stern, A. Kuther, A. A. Gorbunov, A. Forchel, P. Hawrylak, S. Fafard, K. Hinzer, T. L. Reinecke, S. N. Walck, J. P. Reithmaier, F. Klopff, and F. Schäfer, Fine structure of neutral and charged excitons in self-assembled In(Ga)As/(Al) GaAs quantum dots, *Phys. Rev. B* **65**, 195315 (2002).